

Higher order variational denoising for diffusion tensor imaging

Florian Knoll¹, Tuomo Valkonen², Kristian Bredies³, and Rudolf Stollberger¹

¹Institute of Medical Engineering, Graz University of Technology, Graz, Austria, ²Department of Applied Mathematics and Theoretical Physics, University of Cambridge, Cambridge, United Kingdom, ³Department of Mathematics and Scientific Computing, University of Graz, Graz, Austria

Target Audience: The target audience for this work are researchers who are interested in new methods for image enhancement and diffusion tensor imaging (DTI), as well as all users of DTI seeking to reduce data acquisition time.

Purpose: High resolution diffusion weighted imaging (DWI) and DTI with isotropic voxels are desirable for a large number of applications. Unfortunately, acquisitions of such data sets are challenging, due to the notoriously low SNR of DWI. ¹ In addition, even with fast sequences like single shot EPI, measurement times often become prohibitively long because of the large number of diffusion encoding directions that have to be acquired. In this work we introduce two higher-order variational denoising approaches for the reconstruction of DTI data with isotropic voxels from a single average. These are based on Total Generalized Variation (TGV), ² which has the property of preserving edges (between, e.g., white and grey matter), while also correctly restoring smooth areas unlike first-order Total Variation (TV) approaches.

Methods: Two different variational denoising approaches were investigated in this work. For the first approach, the individual diffusion weighted images were denoised prior to calculations of the diffusion tensors:

$$\min_{u_b} \|u_b - A_b\|_2^2 + \alpha TGV^2(u_b).$$

In this equation, A_b is a single, noisy, diffusion weighted image that was obtained without averaging, u_b is the corresponding denoised image, the index b represents the different diffusion directions, $TGV^2()$ is the regularization functional and α is a regularization parameter. In the second approach we model the Stejskal-Tanner equation in the fidelity function. Namely, we solve the diffusion tensor field D from

$$\min_D \sum_b \left\| \log \frac{A_b}{A_0} + b \cdot D \right\|_2^2 + \alpha TGV^2(D).$$

Where A_b is again the DWI measurement corresponding to the gradient b and A_0 is the image without diffusion encoding. In this case the regularization functional $TGV^2()$ is defined in a way that it directly operates in the tensor space of D . We denote this approach as tensor based denoising. For the numerical solution we write both problems in saddle-point form and employ a primal-dual algorithm presented in ³. The regularization parameter is chosen within a preset range to minimize Frobenius norm error to the 9 averages ground truth.

DTI measurements of a healthy volunteer were performed on a clinical 3T system (Siemens Skyra), using a conventional 20 channel head/neck coil. A diffusion weighted single shot SE-EPI sequence was used with diffusion sensitizing gradients in 20 directions ($b=1000s/mm^2$) and one additional scan without diffusion encoding. Sequence parameters were: TR 3700ms, TE 95ms, acquisition matrix 128×128 , 25 slices, in-plane resolution $1.7 \times 1.7 mm^2$, slice thickness 1.7mm, 6/8 partial Fourier in the phase encoding direction and GRAPPA with an acceleration factor of 2 using 38 autocalibration lines. Two sets of data were acquired: In the first measurement, a very high number of 9 averages was used in order to have a high SNR gold standard available for reference. The total scan time of this measurement was 12 min.

Afterwards a second data set was obtained, measuring only a single average with a scantime of 1.5 min. Prior to reconstruction of the diffusion tensor, eddy current correction was performed using FSL. ⁴ Denoising was then performed with the two methods described above.

Results: Fig. 1 displays non-diffusion weighted images and images from three different diffusion directions from a single average, as well as for the measurement with 9 averages. In addition, the results from individual denoising of the single average DWIs are shown. Reconstructions of DTI maps from 9 averages, the single average data set, tensor based denoising of the single average data and individual DWI denoising are shown in Fig. 2.

Discussion and Conclusion: It can be seen from the results that TGV based denoising of measurements with a single average leads to results with an SNR that is comparable to that of 9 averages. In practice, this leads to a significant reduction of scan-time. The price for the SNR gain is a slight reduction of sharp edges and loss of very fine features. This effect can be observed in both individually denoised DWIs and the reconstructed DTI maps, and is slightly reduced in the case of tensor based denoising. It should be noted that while our choice of the regularization parameter ensured that comparable values are used for the two different methods, the minimization of the error norm to the 9 averages data set cannot be considered absolutely optimal because the data sets were acquired sequentially and small movements of the volunteer occurred between the individual measurements.

References:

1. Tournier JD et al. Diffusion tensor imaging and beyond. MRM 65: 1532-1556 (2011).
2. Knoll et al. Second order total generalized variation (TGV) for MRI. MRM 65: 480-91 (2011).
3. Chambolle and Pock. A first-order primal-dual algorithm for convex problems with applications to imaging. J Math Imag Vis: 40, 120-145 (2010).
4. Smith et al. Advances in functional and structural MR image analysis and implementation as FSL. NeuroImage, 23:208-219 (2004).

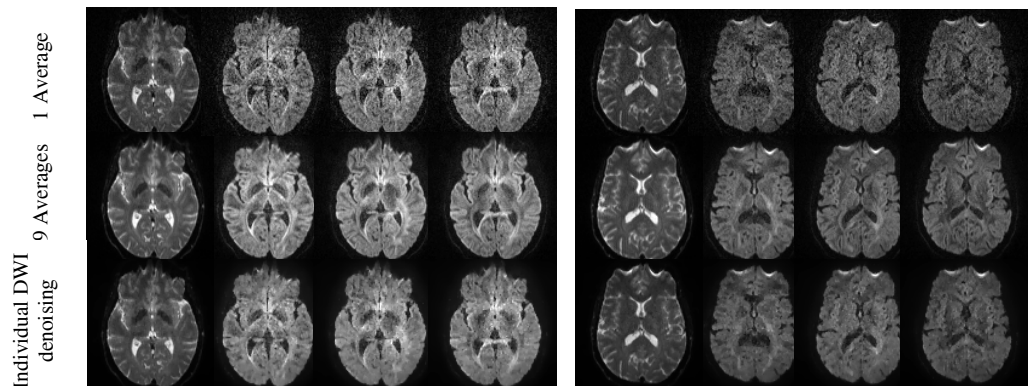


Fig. 1: Comparison of individual diffusion weighted images, non-diffusion weighted and four different diffusion directions are displayed. Measurements using a single average (top row, scantime 1.5 min) and 9 averages (middle row, scantime 12 min) are shown for two different slices. The bottom row contains the results of the TGV based denoising of the single average individual DWIs.

9 Averages 1 Average Individual DWI denoising Tensor based denoising

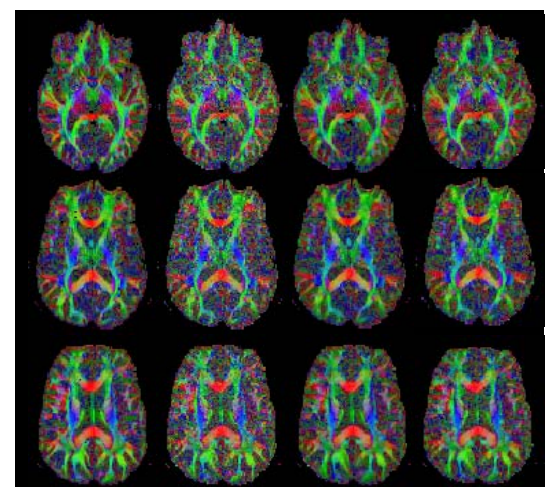


Fig. 2: DTI maps from measurements with 9 averages (first column), a single average (second column), results from a single average after performing individual denoising of the diffusion weighted images (third column) and from Tensor based denoising as described (fourth column).